2015

Left Ventricle Volume Reconstruction to Minimize Scanning Time: Slice-Fitting Method

Prateek Kalra
Wright State University

Left Ventricle Volume Reconstruction to Minimize Scanning Time: Slice-Fitting Method

A thesis submitted in partial fulfillment of the requirements
for the degree of Master of Science in
Biomedical Engineering

by

Prateek Kalra
B.S., University of Minnesota, 2010

2015
Wright State University

Wright State University
GRADUATE SCHOOL

May 11, 2015

I HEREBY RECOMMEND THAT THE THESIS PREPARED UNDER MY SUPERVISION BY Prateek Kalra ENTITLED Left Ventricle Volume Reconstruction to Minimize Scanning Time: Slice-Fitting Method BE ACCEPTED IN PARTIAL FULFILLMENT OF THE REQUIREMENTS FOR THE DEGREE OF Master of Science in Biomedical Engineering.

Nasser H. Kashou, Ph.D.
Thesis Director

Thomas N. Hangartner, Ph.D.
Chair, Department of Biomedical,
Industrial and Human Factors Engineering

Committee on
Final Examination

Kimerly A. Powell, Ph.D.

Arthur A. Goshtasby, Ph.D.

Caroline G.L. Cao, Ph.D.

Nasser H. Kashou, Ph.D.

Robert E.W. Fyffe, Ph.D.
Vice President for Research
Dean, School of Graduate Studies

ABSTRACT

Kalra, Prateek. M.S.B.M.E., Department of Biomedical, Industrial and Human Factors Engineering, Wright State University, 2015. *Left Ventricle Volume Reconstruction to Minimize Scanning Time: Slice-Fitting Method.*

Assessment of left ventricle volume is usually done for diagnosis and prognosis of heart diseases. Slice-summation method is a standard method used to compute left ventricle volume where region of interest from several short axis (SA) slices are added. There are some limitations to this method, however. It requires short-axis slices to be taken parallel to the mitral valve plane from the base to apex. Moreover, scanning several short-axis slices is a tedious and time consuming process especially for studies that require several hundreds datasets. There are some existing methods to reconstruct left ventricle volume but most of them depend on several SA slices for accuracy. The ones that claim to use fewer slices have complex algorithm that can not be easily implemented and customized to individual's application. This thesis proposes a slice-fitting method that can be implemented using MATLAB's Image Processing Toolbox. The slice-fitting method uses one SA slice from the middle region of left ventricle and two orthogonal long axes (sagittal and coronal) slice to estimate volume. The correlation between the volume computed by slice-summation and slice-fitting method is found to be greater than 0.5 and it was when volume estimated by slice-fitting method used only one LA and one SA slice. This report also provides some optimization techniques that can be used to improve the imaging protocol that in turn can make the use of slice-fitting method more efficient.

Contents

List of Figures

List of Tables

Acknowledgment

I would like to thank my advisor Dr. Nasser Kashou for bringing me the right project and guiding me through every phase of it. I like to thank my sister Neha Kalra who connected me with Dr. Kashou in the first place. I also like to thank people (names too numerous to mention) I met who kept my life other than school exciting that it all felt like a piece of cake.

Dedicated to my grandmother, Shanti Devi (goddess of peace)

Chapter1

Introduction

Cardiovascular disease is one of the biggest health problems in the world today. Assessment of left ventricle (LV) in heart is usually done for diagnosis and prognosis. Figure 1.1 shows the heart anatomy and the three reference axes: axial, sagittal and coronal. Cardiac Magnetic Resonance Imaging (CMRI) is widely used to capture the short-axis (SA) and long-axis (LA) slices of LV to quantify volume at end-of-diastole (ED) and end-of-systole (ES) cardiac phases by using a standard method called slice summation technique.

The base or basal region of LV starts at the mitral valve plane (MVP). The apex or apical region is the bottom most of the LV where it gets narrower. The mid or middle region lies between the basal and apical regions.

1.1 Problem Statement

Non-invasive studies on live animals such as mice are the most difficult to perform and they take about one hour of MRI scan time per subject, not including the anesthetic induction and recovery time of animals. However, studies on live animals provide more physiological information than postmortem studies [2]. Scanning becomes significantly more time-consuming and expensive when a study involves several hundred animals.

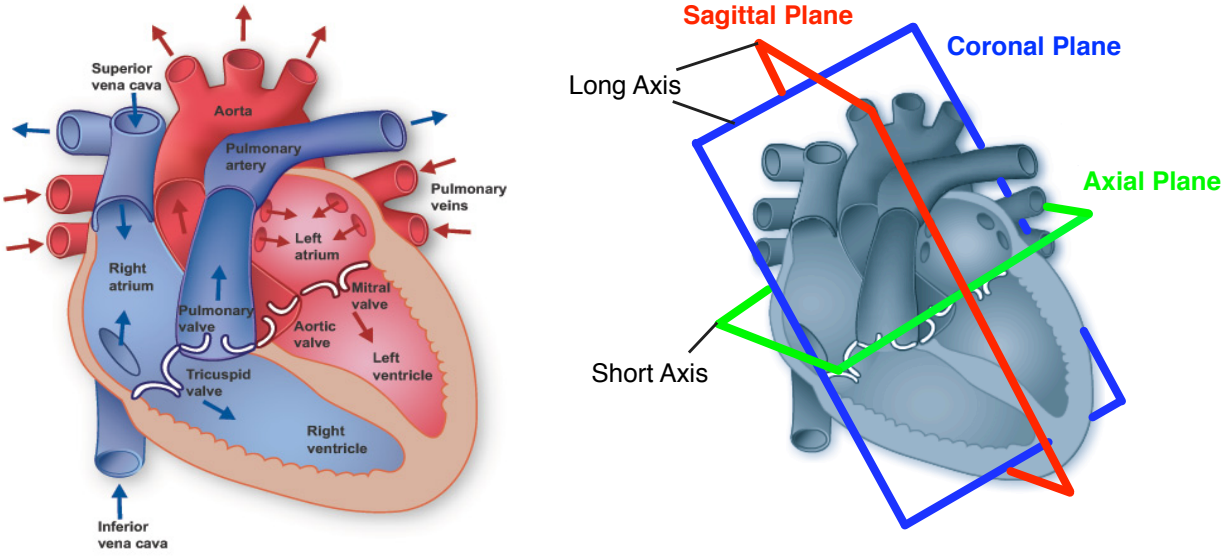

Figure 1.1: (a)Heart image showing 4-chambers view containing left ventricle, left atrium, right ventricle and right atrium. (b) showing long axis planes (sagittal and coronal) and also short axis plane (axial). Heart image is taken from [1]

The problem that we are trying to solve came from a pre-clinical studies on mouse cardiac where setting up a mouse and scanning several slices is a time-consuming process. To overcome this problem, one way is to reduce the number of slices to be scanned. Reducing the number of slices would not only reduce the scan time but also the segementation time for those slices. This would require a methodology that could estimate volume of LV by utilizing only a few slices. This could only be possible if we have a methodology that could perform three-dimension (3D) reconstruction of LV using only a few two-dimension (2D) slices.

Several approaches [3, 4, 5, 6, 7, 8] (discussed in Chapter 2) have been made to reconstruct 3D model of LV using 2D MRI slices. However, most of them requires about 6-8 SA slices to estimate volume, which does not solve our problem as our goal is to reduce the number of slices and hence the scanning time. The ones that claim to use fewer slices have complex algorithm that cannot be easily implemented nor customized for individual applications.

1.2 Significance

In this report, a new method is proposed called slice-fitting method for 3D reconstruction of LV. This method requires one SA slice from the middle of the heart and one or a couple of LA slices depending on the desired accuracy. Moreover, this methodology can be easily implemented using MATLAB's Image Processing Toolbox and can be customized to individual's application. Reducing the number slices would not only reduce the scanning time but also reduce the time consumption in manually segmenting the region of interest in those slices. One could use available automatic segmentation methods [9, 10, 11, 12, 13, 14] but they are sensitive to image quality and as a result, their performance varies from dataset to dataset.

This report compares the LV volumetric results obtained by slice-fitting methodology with the standard slice-summation technique on datasets from a mouse cardiac MRI study. In addition, it also discusses some of the main concerns addressed in already existing methods and suggests some optimized scanning techniques that could be used in future to improve imaging protocol in order to make an efficient use of slice-fitting methodology to estimate LV volume.

1.3 Hypothesis

The shape of the left ventricle is approximately uniform from base to the middle while begins to narrow at apical region. In SA slices taken using MRI, it is easy to segment the epicardium and endocardium boundaries from the slice taken at the middle of the heart as compared with the basal or apical region.

As there are 360 different angles at which left ventricle can be sliced along the LA, samples taken horizontally from one LA can give the size of the missing SA slices at one angle. Assuming that the size of SA slices is changing uniformly in all angles or directions,

a stack of SA slices can be generated using the information from the samples of LA. Putting a stack of SA slices together in space would give a 3D model of left ventricle.

Volume estimated using slice-fitting methodology is expected to give the same volumetric trend among the datasets as given by standard slice summation technique, which means that the volume numbers would not be the same but the factor by which volume from one dataset changes to the volume in other datasets is expected to be the same in both the techniques.

1.4 Thesis Outline

The Chapter 2 will give some background information on MRI, CMRI, given datasets, region of interest, parameters of interest, slice summation technique and existing methodologies for 3D reconstruction of LV. After talking briefly about the existing methods, strengths and limitations, a new methodology called slice-fitting will be introduced in Chapter 3. Later, chapter 3 will cover mostly the fundamentals behind the slice-fitting method using a uniform shape (ellipsoid) phantom and a non-uniform shape phantom created from a real dataset. Chapter 4 will show the volumetric results of the slice-fitting method and validate through both quantitatively and qualitatively and later will compare the results with the given volume numbers from slice summation technique. Chapter 5 summarize the method, discussing some of its limitations and future work.

Chapter 2

Background

2.1 Magnetic Resonance Imaging

The functioning of Magnetic Resonance Imaging (MRI) is based on the Nuclear Magnetic Resonance (NMR) technology that depends on a fact that body contains water which consists of hydrogen atoms or protons. Proton has a spin magnetic moment and in the presence of a strong external magnetic field, the protons in the body lines up along the direction of magnetic field. Different parts in body like soft tissue, bone etc. have different protons concentration. When a radio-frequency (RF) signal is send to the selected region (the region of interest), it gives energy to proton and flip its direction of spin. When the RF signal is stopped, the protons in the selected region relaxes back to normal, back to the direction of magnetic field and releases the extra energy in the form of a RF signal, which is then recorded by a computer. In order to determine the location of the different tissues or structures, a magnetic field gradient (in addition to the strong magnetic field) is set across the region of interest. The resulting output signal is converted into Fourier transform where different frequency components are isolated that determines the location of the object while comparing with the gradient field strength at that location. In order to capture the region of interest from different angles, RF signal is transmitted and detected about 360 degrees

around the region of interest.

2.2 Cardiac MRI

Cardiac MRI (CMRI) is used for various applications such as assessing myocardial mass and volume, flow of blood in vessels, to detect the presense of coronoary artery disease, myocardial scar and perfusion imaging, stress imaging and tumors [15].

The heart beats about 60-100 times per minute in humans and about 300-600 times per minute in mice. MRI systems are not fast enough to capture all the cardiac phases in just one cardiac period and causes motion artifacts. In order to eliminate motion artifacts due to movement of heart when it's beating is done by triggering the MR scanner using an electrocardiogram (ECG) gated signal. An ECG signals shows the cardiac cycle where the R-R interval determines the heart beat rate. With each beat, heart goes through one cardiac cycle which involves expansion and contraction of LV to its extremes. For ECG gating, one RR interval is divided into several segments and labeled.

Because the heart is beating too fast, MR image is obtained over several cycles and reconstruction is done using the same segment from several cardiac cycles. This produces a series of images for all cardiac phases. When these images are viewed or played together, they represent the motion of heart for that slice like a movie. This method is called CINE MRI.

As shown in Figure 2.1, CMRI is taken at three different planes: 1. Sagittal, also called 2-chambers view as it contains left ventricle and left atrium. 2. Coronal, also called 4-chambers view as it contains left ventricle, left atrium, right ventricle and right atrium. 3. Axial, the cross section view that contains left ventricle and right ventricle. Sagittal and coronal are long-axis views that are orthogonal to each other and axial is a short axis view.

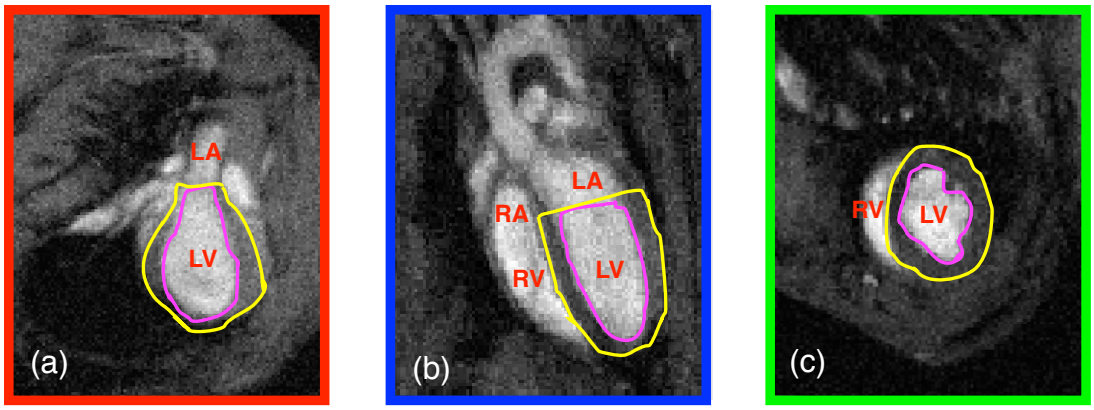

Figure 2.1: Slices taken from mouse cardiac at ED phase. a) showing the sagittal, a 2-chamber view containing left atrium (LA) and left ventricle (LV). b) showing the coronal, a 4-chamber view containing right atrium (RA), right ventricle (RV), LA and LV. c) showing axial or SA view. Regions of interest: Epicardial boundary is the outer boundary (yellow) and endocarial boundary is the inner boundary (pink).

2.3 Given Datasets

The given datasets came from a mouse cardiac MRI study performed at Ohio State University (OSU). MRI images were taken using 11.7 T MRI system from Bruker for small animal imaging. Each dataset contained several (about 6-8) SA slices and one LA (coronal) and in some datasets two orthogonal long axes (coronal and sagittal) taken at both the ED and ES phase of cardiac cycle.

2.3.1 Image Acquisition Parameters

The image quality depends on many factors like echo time (TE), repetition time (TR), the number of signal averages (NA) and resolution. Increasing TR increases scanning time. Decreasing TR would decrease the scanning time but at the expense of low signal to noise ratio (SNR) [16]. For the given datasets, TR is 8 ms, TE is 1.4 s, fractional anisotropy (FA) is 15 degrees, slice thickness is 1 mm with field of view (FOV) is 30 mm x 30 mm and matrix size 256 x 192. The in-plane resolution is 115-150 micro meter. The given SA slices are numbered 1 through 7 or 8 ordered from apex to base of LV. These parameters

were defined and set the same throughout the data acquisition for all datasets. This ensures that the image quality is expected to be equal for all datasets.

2.3.2 Imaging Protocol

A scout image of coronal long axis was produced to make sure the region of interest lies in the field of view. This is also used to test the exposure technique and to set a baseline or reference for taking SA slices. Once scout image is taken, a line is drawn connecting the center of ascending aorta and the center of the apex. Ideally, the SA slices are to be taken parallel to mitral valve plane (MVP) in order to be consistent throughout the datasets. However, the given SA slices are taken based on the sagittal and coronal axis views.

2.3.3 Time Consumption

The scan time was about 6 minutes per slice. The total time to acquire one dataset was about 1 hour that consists of about 6-8 SA slices and two LA slices. Post processing took about 10 minutes per dataset where regions of interest in SA slices are segmented and volume number is generated by summing SA slices.

2.4 Regions of Interest

Endocardium boundary: It is the inner most boundary of the left ventricle that defines the LV cavity or blood pool. Region of interest involves the endocardium boundary at both ED and ES phase. Figure 2.1 shows the endocardial boundary highlighted in pink.

Epicardial boundary: It is the outer most boundary that defines the outer boudnary of myocardial muscle surrounding the LV cavity. Region of interest involves the epicardium boundary at ED phase. Figure 2.1 shows the epicardial boundary highlighted in yellow.

2.5 Parameters of Interest

Left Ventricle Mass: At the ED phase of cardiac, subtracting endocardium volume from epicardium volume will give volume of left ventricle muscle or myocardial muscle, which is then converted into unit of mass by multiplying with the specific myocardial density that is 1.05g/cm-cube and give left ventricle mass (LVM) as shown in Equation 2.1 below:

$$LVM = Myocardial\ Muscle\ Volume \times Myocardial\ Density \tag{2.1}$$

Ejection Fraction: Segmentation of endocardial boundary at the ED phase gives end-of-diastole volume (EDV) and at ES phase gives end-of-systole volume (ESV). Ejection fraction (EF) is the fraction of blood that is ejected out per EDV when heart goes from ED to ES cardiac phase as shown in Equation 2.2 below:

$$EF = \frac{(EDV - ESV)}{EDV} \tag{2.2}$$

Relation between LVM and EF: Both the parameters, LVM and EF are used for prognosis and diagnosis of heart diseases. There are studies [17, 18] that show an inverse relation between LVM and EF as shown in Equation 2.3. More the LVM, less is the EF. Another study [17] found that there is 1.22 times relative risk of death for each 50g/m increase in LV mass index. A study on Hypertrophy [19] talked about how the heart changes its LV mass in response to the external stress and found that the myocardial walls become thick to bear stress load.

$$EF \propto \frac{1}{LVM} \tag{2.3}$$

2.6 Slice Summation Technique

The standard method used to compute LV volume is called slice-summation technique. Based on this method, the regions of interest in several SA slices are segmented and summed together to compute volume. Scanning several SA slices is very tedious and time consuming process however. The time consumption become especially significant in case of pre-clinical research studies where a large number of dataset is being analyzed to make inferences. This also adds up to the cost, usually the cost for using MRI system. Moreover, there are some limitations to the standard slice-summation method. For accuracy and consistency, SA slices should be taken parallel to MVP and from base to apex of the ventricle. Also this method involves human intervention while defining a plane for SA slices and their accuracy depends on experience level of data collector which questions the repeatability of collected data.

2.7 Existing methods for left ventricle reconstruction

This section contains a brief overview of some of the existing methods for LV 3D reconstruction. This would help to focus on some crucial things by learning from both, the strengths and the limitations of each of the existing methodologies.

Left ventricle geometry in rats: Left ventricle geometry has been investigated during systole and diastole in rats using MRI [5]. The goal of this study was to minimize imaging time by using fewer slices. Quantitative models (elliptical, quartic and parabolic) were developed and fit analytically to the stack of short axis slices. The outcome of this method was that the elliptical model gives more even qualitatively acceptable fit and it was only in diastole. The limitation of this approach is that it requires more control points means more SA slices to get accurate fit and hence accurate volumetric results.

Curvature based approach for shape analysis: In this study [4], shape of the heart is analyzed while going from ED to ES phase in both normal and diseased heart in humans based on the surface curvedness in different regions (base, mid and apex) of the heart. Several SA slices and LA were used to reconstruct 3D surface for accuracy and the human intervention was involved for manually segmenting the region of interest in SA slices and placing control points. The major finding of this study was that the curvedness in each region of normal heart was higher as compared to diseased heart at both ED and ES cardiac phase. Moreover, the change in the curvedness while going from ED to ES was found to be the largest in the apical region of normal heart and that may be due to functioning of normal heart to its full extreme when the LV is contracting.

Feedback assisted 3D reconstruction: This study [6] utilized two orthogonal long axis and about 8-10 short axis slices to construct 3D model of left ventricle. This study shows that the misalignment in the SA plane while scanning can produce significant variability in the results of LV volume and mass. The limitation of this method is that it depends on more number of slices for its accuracy.

Super-ellipse fitting method: This method [8] is based on fitting super-ellipse to the stack of short axis slices with excellent accuracy due to ellipsoid shape of LV. This confirms the outcome of previous study [5] about left ventricle geometry in rats that the LV has an ellipsoidal shape during ED. One of the limitations was that it was hard to fit papillary muscle in the super-ellipsoidal model and that's why they considered papillary muscle as the part of blood pool instead of a part of myocardial muscle.

Fusion of short axis and long axis: This methodology [7] uses a fusion of 8 SA slices along with a sequence of LA images and perform voxel interpolation to reconstruct LV in high resolution. Again the accuracy of volume depends on several number of SA slices along with LA slices.

Combining long and short axis MR images: This paper [3] uses two orthogonal (sagittal and coronal) LA slices to get information about the position and orientation of mitral valve plane, apex, endocardial and epicardial contours. Intersection points of intersection planes and two orthogonal LA slices were used as control points and interpolation is done based on the pixel value of the adjacent SA slices.

2.8 Inferences on the outcomes of existing methods

Although we learnt a lot from the strengths and limitations of the existing methods, none of them really solve our problem. Most of the existing methods discussed in previous section rely on several SA slices for their accuracy. Moreover, the one that only uses few SA slices (as in [5]), fail to estimate LV volume at ES phase. Some of the information obtained from the existing methods, which we may use to develop our methodology are: 1. LV has an ellipsoid shape which is usually true for ED phase. 2. For normal heart while going from ED to ES, the apical region has the largest change in curvedness. 3. Papillary muscles is included in the LV or not, should be stated clearly as it would make a difference in volumetric calculations. 4. Use of both SA and LA slice would give more accurate volume.

Chapter 3

Methodology

3.1 Segmentation

The segmentation was done manually using MATLAB's Image Processing Toolbox. Since the goal is to reduce the number of slices, the automatic segmentation is of no interest. There are some existing automatic segmentation algorithms [9, 10, 11, 12, 13, 14] but they are sensitive to image quality and cannot be used for every dataset. To make the manual segmentation process faster and convenient to use, a Graphical User Interface (GUI) was built using some basic image editing functions in MATLAB like thresholding and binary mask plus some editing features like adding and deleting.

Figure 3.1 shows six SA slices from one of the given mouse cardiac MRI datasets at ED phase. Here, we have six SA slices. Using manual segmentation GUI, epicardial boundary was segmented. The segmented boundaries of epicardium were then converted into a binary mask. After obtaining the binary masks of each SA slices, contours were drawn at the boundary of each mask. As the LA of LV is not parallel to vertical axis, the given slices centers were not common. In order to observe the trend in the variation in the size of the given SA slices while going from apical to mid to the basal region of LV, the contours of SA slices were forced to have a common center and grouped together as shown

in the top half of the Figure 3.1. Here, the SA slices are ordered from apex to base and numbered from 1 through 6 respectively. Later, the trend is compared with the slices taken from an elliptical model and grouped in similar way as shown in the bottom half of the Figure 3.1.

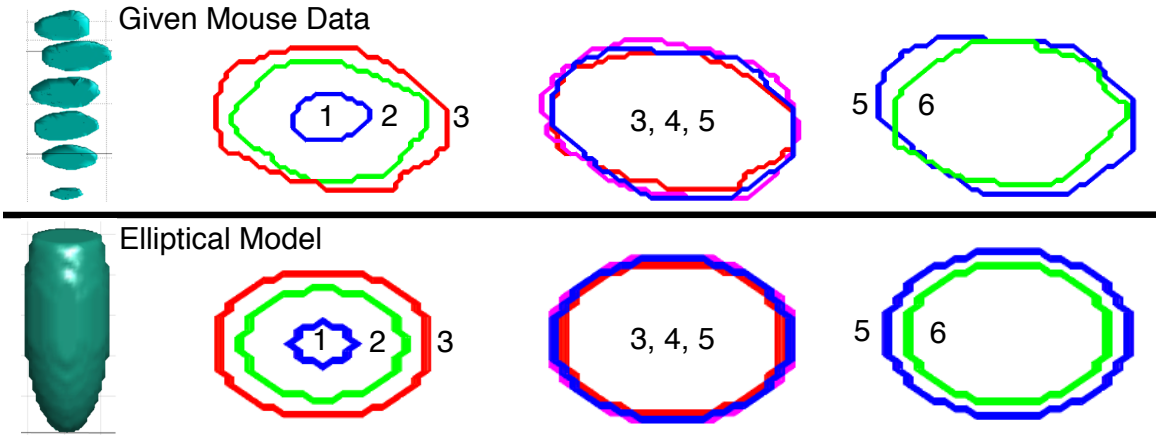

Figure 3.1: Top half contains SA slices from given mouse data at ED phase made to have common center and classified into three groups representing apical, mid and basal region of LV.Bottom half contains SA slices taken from an elliptical model(generated in MATLAB) and used as reference for comparison with given mouse data.

The first observation made is that the size of the masks in the middle region (3,4,5) is approximately similar in all given datasets. See Appendix A for several other datasets SA contours. This means that we can approximate the mid region of LV by using only one SA slice taken at the mid region of LV. Second observation is the rate of change of size of the short axis slices in both the apical (1,2,3) and basal (5,6) regions are approximately the same in all directions just like in elliptical model. Based on these two observations, one can get information about not only the shape of the ventricle but also how the size is varying among other SA slices taken perpendicular to LA. Shape of the LV is determined by taking a SA slice from the middle of the heart. Size variation among SA slices can be determined by size variations in the samples of LA slice going from center of base to the center of apex. If we assume that the size of SA slices is varying uniformly in all directions, one can use one LA slice going from base to apex and one SA slice from the middle regin

to estimate the LV volume.

3.2 LV Reconstruction using Slice-Fitting Method

In order to estimate volume, slice-fitting method is proposed that will generate a stack of SA slices from one given SA slice and fit them appropriately in 3D space based on the information from the samples of one given LA slice. This methodology is not only easy to implement using Image Processing Toolbox in MATLAB but also provide accurate results for LV volume estimation.

In this section, we begin with understanding the slice-fitting methodology by applying it on a half-ellipsoidal phantom made to approximate the LV shape. Later, we include the same phantom but at an angle to see if we can estimate the volume using the same methodology. This would also tell us what measures can we take to improve the imaging protocol to make it independent of the determination of SA plane that would later help in making the use of this methodology more efficient. Towards the end of this section, we will estimate the volume of a non-uniform shape phantom, which is actually the shape of LV at different phases of cardiac.

3.2.1 Phantom (unrotated)

In order to understand how 3D volume is reconstructed using one LA slice and one SA slice, a phantom was created in MATLAB using Image Processing Toolbox by cutting an ellipsoid object into half as shown in the Figure 3.2. Using this phantom as a reference object, whose volume is known, we taken an SA slice and an LA slice from it. Using the SA slice and LA slice from phantom as our inputs to the slice-fitting methodology, we reconstruct a 3D object and compare its volume with the reference phantom volume, both quantitatively and qualitatively.

The LA slice is the taken vertically (highlighted with red boundary) at the center of the base to the center of the apex so that we can get a full 2D profile of the phantom. The SA slice is taken horizontally (highlighted with black boundary) somewhere from the middle of the phantom. The reason for choosing SA slice from the mid region of LV is that in the given dataset, it is easier to visually distinguish and segment the region of interest in SA slice taken from the mid region as compared to the basal and apical region of LV. In addition, the mid region is the major part of ventricle (as it closely approximate the basal region as well) and so taking a SA slice from mid region is expected to give a more accurate estimation of LV volume.

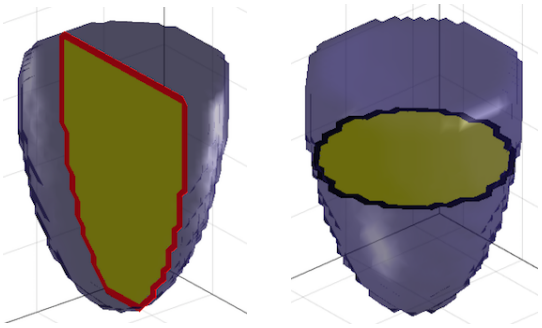

Figure 3.2: LA slice (in red) taken vertically at the center of base to the center of apex. SA slice (in black) taken horizontally at the mid region of phantom.

As shown in Figure 3.3, when an image is loaded in MATLAB, it treats the image as a bunch of rows (horizontal) and columns (vertical) with various intensity values. The smallest block in a matrix is called pixel and there is a specific intensity value associated with each pixel in an image. When a binary mask of SA slice, that consists of only high intensity (white) and low intensity (black), is loaded into MATLAB, it's shape is no more circular or ellipse but it becomes blocky at the edges. The size of the given SA slice can be determined by the dimension of the bounding rectangle around it with unit in pixels.

With LA slice in the form of matrix in MATLAB, the number of rows the high intensity region has, equals the number of 2D SA slices needed to generate 3D volume.

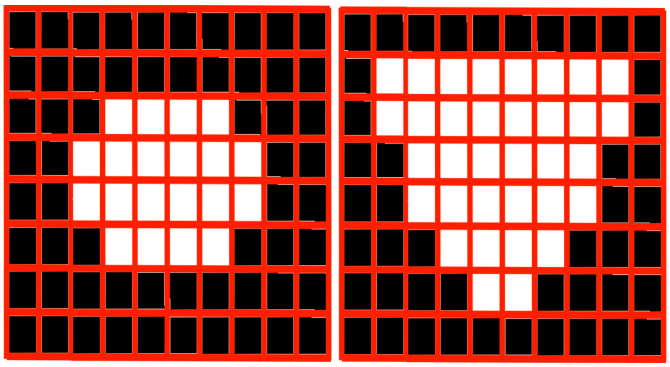

Figure 3.3: Binary mask of SA (on left) and LA (on right) shown in the matrix form in MATLAB. Size of the SA is determined by the number of rows(length) and columns(breadth). Number of rows in LA determines the number of SA slices required to generate volume.

Sampling the given LA slice horizontally would give the samples row wise. By calculating the number of high intensity pixels, we can find the dimension of the samples of LA. One of the LA samples dimension matches roughly with one of the dimensions (length or breadth) of the given SA slice as the two slices SA and LA were taken from the same phantom to begin with.

Knowing how the size of samples of LA is varying as compared to the fixed given SA slice, one can resize the given SA slice and create a stack of missing SA slices. Moreover, the shift in the centers of samples of LA as compared to given SA slice center, determines the placement of the stack of SA slices in space in order to get an approximate shape of LV. Although, the volume is determined by the summing the stack of generated SA slices which would not change even if they are shifted in space, the shift is required to estimate the shape of the phantom we began with and will help in qualitatively validating the methodology by comparing the estimated 3D phantom shape with the shape of the given 2D LA slice.

Image resize and image shift functions are used in MATLAB to perform image resizing and shifting. Image resize function provides two degree of freedom (horizontal and vertical) in which the given image can be resized. As we assumed that the shape of LV can be approximated with elliptical model where the dimension of SA slices varies uniformly

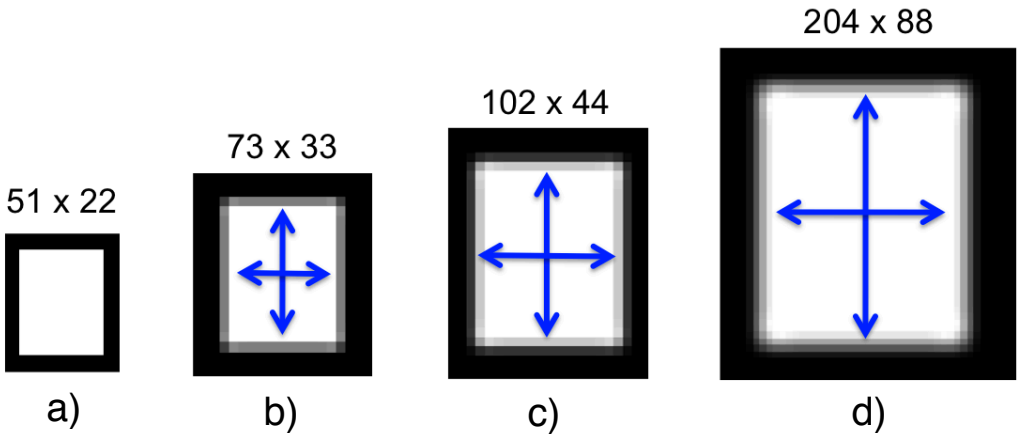

Figure 3.4: Use of the image resize function in MATLAB to resize a given mask by the same factor in both directions.

in all directions, we can use image resize function to resize equally in both possible directions which results into resizing uniformly in all directions in MATLAB. Figure 3.4 shows how the given SA slice can be resized to any scale factor efficiently in all directions.

As we see in Figure 3.5 (a), when the given SA slice is resized, the size of the output image changes. In order to create a volume, all the SA slices are made of same size (determined by the size of the largest SA slice generated) and are centered. At this point, if there is any shift in the center of the samples of LA, the generated stack of SA slices are shifted appropriately using image shift function which allows the shift without changing the size of the output image as shown in Figure 3.5 (b). However, we need to make sure that the shift is not making the region of interest go out of the image boundary. Otherwise, it will result into a cropped image.

In Figure 3.6, we can see that we get about thirty samples (only multiples of 5 shown) as green horizontal lines. Size of each of these samples corresponds to one of the dimensions of missing SA slices. Since the SA slices were taken from an ellipsoidal phantom that grows uniformly in all directions, knowing the change in the size in one dimension, we can generate missing SA slices by resizing the given SA slice uniformly in all directions.

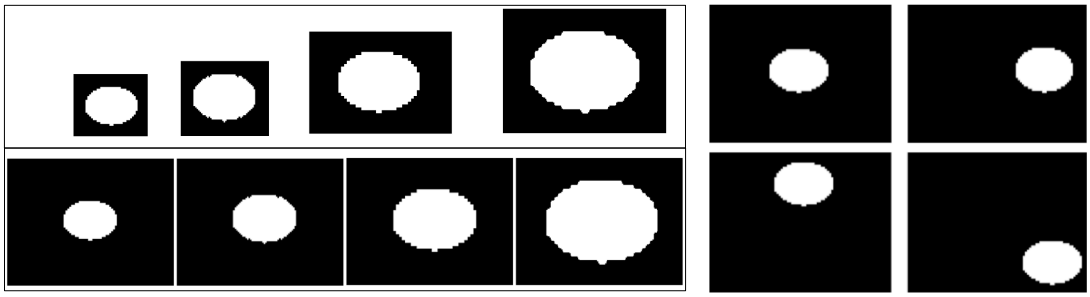

(a) Image Resize (b) Image Shift

Figure 3.5: (a) In top half, image resize function is applied on an ellipse to generate ellipses of different size growing uniformly in all directions. In bottom half, the generated slices are made of same size and high intensity region is centered.(b) Use of image shift function in MATLAB on an ellipse. The size of the output image remains the same.

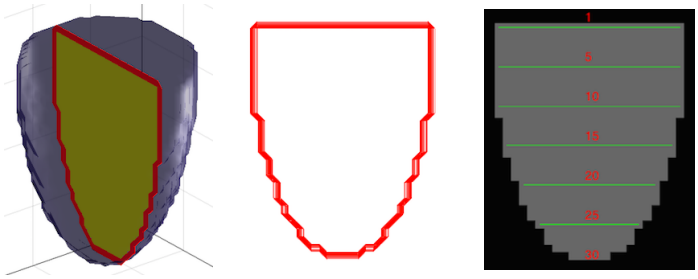

Figure 3.6: Samples of LA slice taken represented by green horizontal lines and numbered from first high intensity row to the last high intensity row.

In this example, we would need thirty SA slices to generate volume.

The flow chart in Figure 3.7 demonstrates the flow of major functionalities involve in slice-fitting methodology. Binary mask of one SA slice and one LA slice are the only two inputs. Samples of LA slice are obtained by extracting all the rows in binary mask of LA and finding the first and the last row that has non-zero size or number of high intensity pixels. This results into an array containing each sample dimension and center coordinate. The size of the given SA slice is determined and a row level is set by manually looking at the size of samples of LA that closely matches with one of the dimensions of given SA slice. Keeping given SA slice as a reference, an array of scale factors is determined by dividing each samples size by the size of given SA slice. Using scale factors as inputs to image resizer along with the given SA slice, a stack of SA slices is generated by resizing

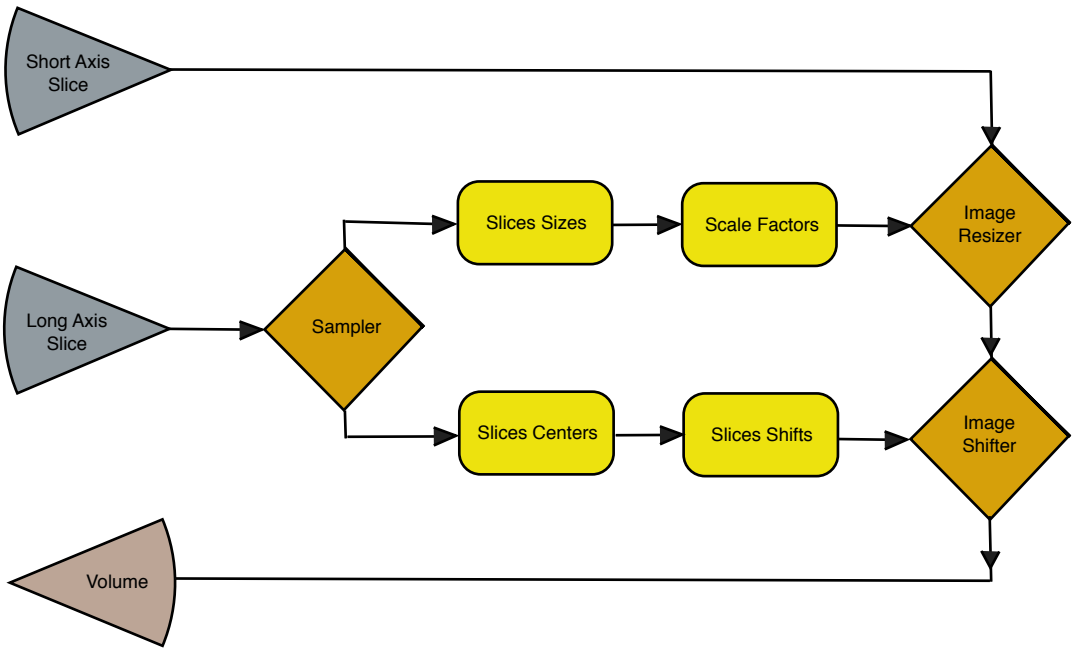

Figure 3.7: Flow chart of slice-fitting methodology.

the given SA slice for each LA sample.

Once the SA slices are generated, next step is to place them appropriately in space. To do that, we use slices shifts array which is generated by considering the center of the top most sample from LA slice as a reference and the shifts in centers of other samples is computed relative to the center of the reference sample. Slices shifts and the stack of SA slices are given as inputs to image shifter to shift the slices appropriately to generate the exact shape of the 3D model. Slices shifts would be zero in the case of phantom where the vertical line passes through the center of the phantom. However, there would be some shift in the samples of LA that is taken from a phantom that is at an angle with respect to the vertical line, which is described in the next section.

3.2.2 Phantom at an angle

In the previous section, we discussed the volumetric method for phantom having center line aligned with the vertical axis. However, this is not the case in real scenario where the

orientation of LV is not known until a scout image is taken. Even the scout image produced is not the best approximation of LA from the center of base to the center of apex. In this section, we would explore some factors that come into picture while estimating the volume of a phantom when the center line going from base to apex is at an angle with respect to the vertical axis.

If we look at the Figure 3.8 of a phantom at an angle, there is no way one can obtain a LA slice going through the center in one go without changing the vertical axis orientation. Since the volumetric method discussed in the previous section depends solely on the LA slice for the estimation of missing SA slices, getting a LA slice form base to apex is crucial in order to get the best estimation of volume.

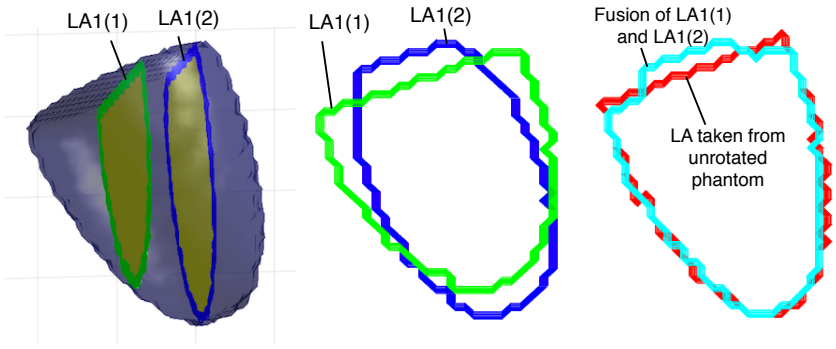

Figure 3.8: More than one LA slices taken for a phantom at an angle to estimate LA from center of base to center of apex. LA1(1) is the LA in green that pass through the center of base but not apex. LA1(2) is the LA in blue that pass through center of apex but not base. Overlaying the two long axes LA1(1) and LA1(2) gives cyan color boundary which is then compared with the red boundary that came from rotating the LA taken at unrotated phantom as shown in Figure 3.6

Multiple LA slices are taken at two different locations in case of phantom at an angle as shown in Figure 3.8. LA1(1) is the LA in green that pass through the center of base but not apex. LA1(2) is the LA in blue that passes through center of apex but not base. None of the two depicts the LA taken from base to apex just by itself. However, when we overlay the two LA slices, it gives us close approximation to the LA taken from base to apex. The two LA slices are fused (in cyan color) and compared with the LA slice (in red)

which was taken directly from an unrotated phantom as shown in Figure 3.6 and rotated by the same angle as in the phantom at an angle. If we manually, delete the hump at the base in the overlaid image of two long axes, it would give us a perfect estimation of LA from base to apex. Based on this observation, one can optimize the LA from base to apex by taking multiple LA of LV at different locations covering both the center of base and center of apex. By following this imaging protocol, there is no need to change the scanning plane angle for LA or SA. It stays the same (horizontal for SA and vertical for LA) in either case (phantom unrotated or phantom at an angle) and makes the imaging process independent of the determination of scanning planes.

Although the slice generated in phantom at an angle would give the same volume as defined by the stack of SA slices generated, SA slices are shifted along the center line to get the exact volume shape for validation purposes. Based on the observations made in this section, if one wants to get an accurate estimation of volume for a phantom at an angle, one must use more than one LA slice taken at different location near the center.

In Figure 3.9, a stack of SA slices is generated by resizing the given SA slice (highlighted in red) based on the samples of the given LA slice. Whether the phantom is rotated at an angle or not, the slice-fitting methodology works efficiently in creating slices and fitting them appropriately. Also the shape of the 3D object generated by slice-fitting method matches closely to the shape and orientation of the given LA slice.

3.3 Real Data Volumetric

In case of ellipsoidal phantom discussed in previous section, the LA view remains the same if seen from any angle about the z-axis. However, this is not true for actual LV shape. To closely approximate phantom with the LV shape, we have created an object using two orthogonal LA slices along with one SA slice taken from one of the given mouse cardiac MRI dataset. Since we do not know the volume of the actual object being compared,

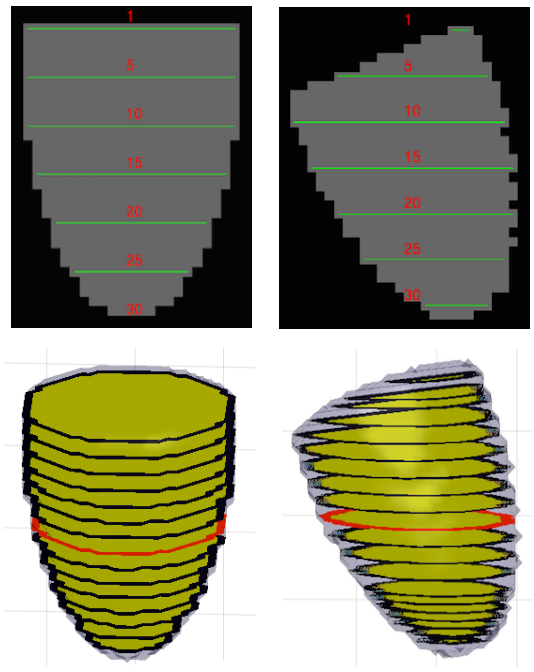

Figure 3.9: Stack of SA slices generated based on LA slice samples. Slice-fitting method is independent of the orientation of phantom and produces 3D output that closely matches with the shape and orientation of given LA slice.The given SA slice is in red outline, while others are generated using Slice-fitting method.

we used this non-uniform 3D object as a reference and went backwards to see if we can generate the same object just like we did in phantom example discussed earlier.

Since LA shape is different while looking at two orthogonal LA views of non-uniform phantom, we will consider two orthogonal LA slices and one SA slice to estimate volume.

3.3.1 Volumetric using two orthogonal LA slices and one SA slice

The assumption we made about the uniform variation in the SA slices in all directions does not hold true in real scenario where ventricle shape is changing from one cardiac phase to another and differs from basal to apical region. For example, as shown in the figure 3.10 and figure 3.11 the two orthogonal view of an object. In this case, if we need to get accurate volume, we need to consider two orthogonal LA slices and resize the given SA slice differently in two directions based on scale factors generated for two orthogonal LA

slices. Moreover, to approximate the LA slice from base to apex, we need to take multiple LA slices and overlay as discussed in earlier Section 3.2.2.

Figure 3.10 shows the one LA view (sagittal) of the non-uniform 3D object which created by taking multiple LA slice of the phantom at different locations and overlaying them. Similarly, in Figure 3.11, where the orthogonal LA view (coronal) of the non-uniform 3D object is created and shown. Note that the number of samples in each LA view is about the same which confirms that the estimated two orthogonal LA profiles are actually taken from base to apex as both should be equal in height.

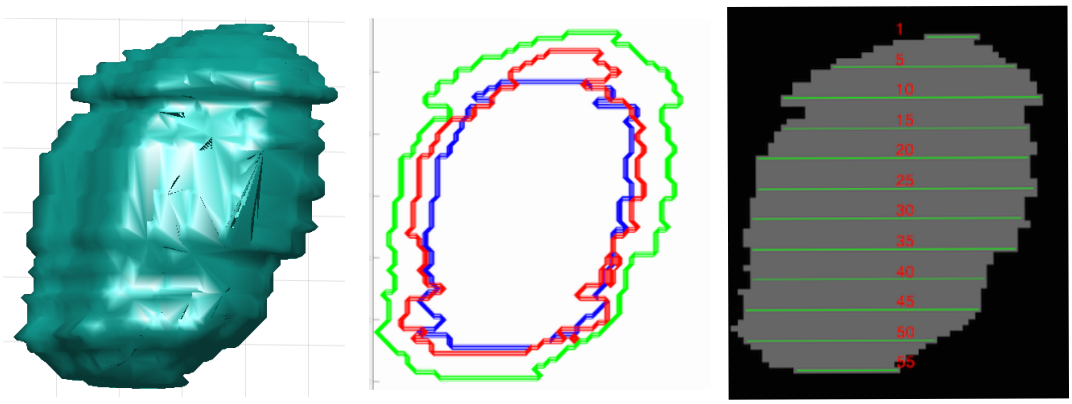

Figure 3.10: Multiple LA (sagittal) were taken at different locations and fused to estimate LA from base to apex.

The flow chart for slice-fitting method is extended to take two orthogonal LA slices and one SA slice to generate volume as shown in Figure 3.12. Here, the image resizer function resize the given SA slice in one direction first based on the sagittal LA samples. The stack of slices created goes to image shifter where the centers are shifted appropriately in the other direction. After that, the generated stack of slices are given as input to the second image resizer function which consider the samples from coronal LA and resize the stack of SA slices appropriately. After going through the image shifter function, it gives the final output which closely depicts the non-uniform phantom object that we began with.

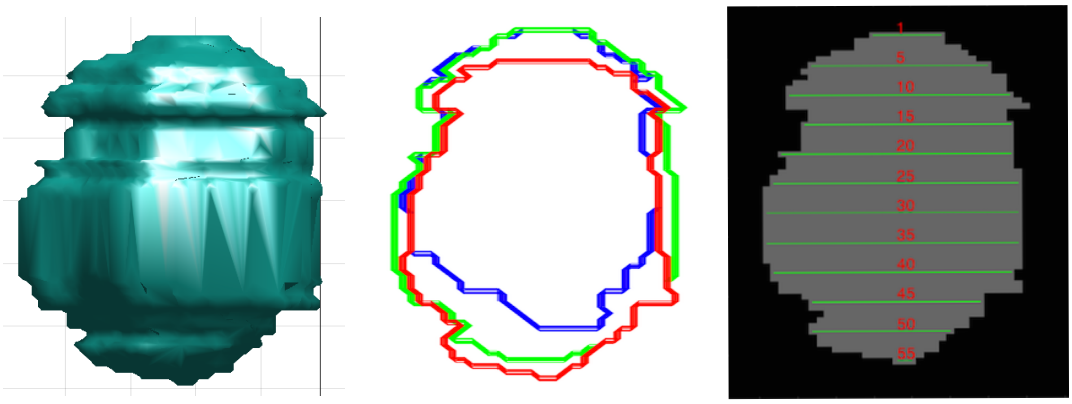

Figure 3.11: Multiple LA (coronal) were taken at different locations and fused to estimate LA from base to apex.

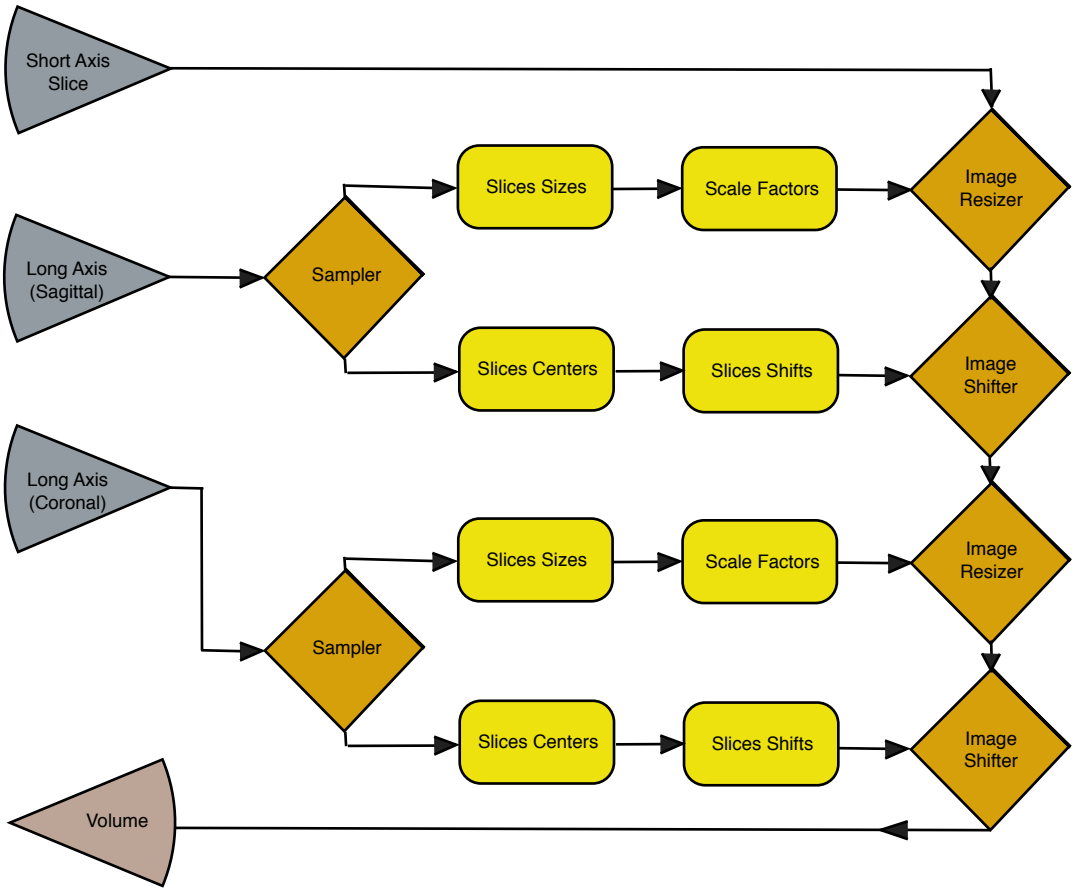

Figure 3.12: Generating volume using two LA (sagittal and coronal) slices and one SA slice (extension of slice-fitting methodology).

Chapter 4

Algorithm Simulation and Testing

In this chapter, we will estimate volume for the phantom (unrotated), phantom at an angle, non-uniform phantom and given datasets as discussed in previous chapter using the slice-fitting methodology and compare the results with the given reference volume numbers. A Graphical User Interface (GUI) is built to make the process of estimating volume fast and convenient. Volume is shown in the number of pixels which can be converted into the desired unit later as per the relation below:

$$VoxelSize = X \times Y \times Z \tag{4.1}$$

where X and Y are the pixel spacing in x-direction and y-direction while Z is slice thickness in z-direction.

$$Volume = Numberof Pixels \times VoxelSize \tag{4.2}$$

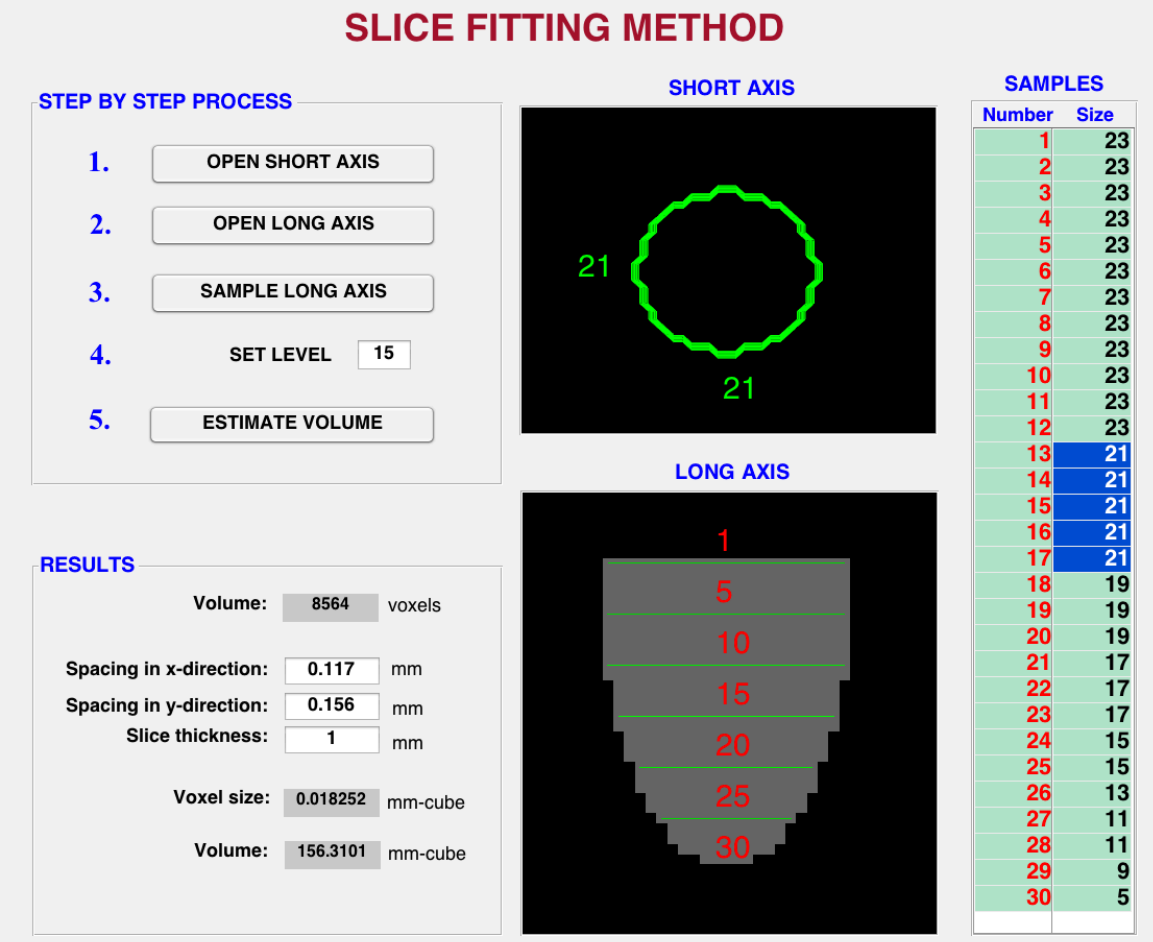

Figure 4.1: GUI built for volumetric computation.

4.1 GUI for Slice-Fitting Method

Figure 4.1 shows the GUI built for implementing the slice-fitting method to estimate volume using one SA and one LA slice. The whole process contains only five steps. First, user loads the binary mask of SA slice by pushing OPEN SHORT AXIS button. Once the SA slice is loaded, it shows its dimensions, length and breadth in terms of pixels. In this example, 21x21 SA slice is loaded. After that, binary mask of LA slice is loaded using OPEN LONG AXIS button and then SAMPLE LONG AXIS button is pressed to sample the binary mask of LA horizontally starting with the first non-zero row until the last non-zero row. Here, about 30 samples of LA are present and each of their dimension is shown in the right most table. Important thing to notice is that for sample number 13 to 17, the

size is 21 which matches with one of the dimensions (length or breadth) of SA slice. SET LEVEL number could be set at any number from 13 to 17 and it will give the same volume results for any number in that range. For instance, 15 is chosen for SET LEVEL. Finally, the ESTIMATE VOLUME button is pressed that follows the slice-fitting methodology in order to create a stack of SA slices and shift them appropriately in space to estimate volume in terms of number of pixels. It will also show a 3D volume output using sliceomatic, an in-built function in MATLAB.

4.2 Validation

To validate the estimated volume, we consider two factors: Number of pixels (quantitative) and the shape (qualitative) of the output that is compared with the known reference volume pixel number and the shape of the given LA slice.

4.2.1 Quantitative: Percentage error difference

Table 4.1 shows the reference volume, estimated volume and error in terms of number of pixels. Reference volume is the volume of phantom object created in MATLAB whose volume is known. This reference volume number is compared with the estimated volume generated using slice-fitting methodology. Error is the percentage error difference between the reference and estimated volume.

In case of phantom unrotated, 6.9 percent fewer pixels found in the estimated volume. In the case of phantom at an angle, where we began with taking multiple LA slices to get an estimation of LA from base to apex, we can see that how the error is reducing as we consider more number of LA slices to generate volume. However, the error number could be misleading by itself. For example, if we compare the error in LA1(1) fused with LA1(2) (uncorrected) and LA(1) fused with LA1(2) (corrected), looking at just the error number,

Table 4.1: Reference volume, estimated volume and error calculations for phantom unrotated, phantom at an angle and real data simulation (non-uniform phantom). Here, we compare the volume in terms of number of pixels to validate quantitatively.

	Reference Volume (in pixels)	Estimated Volume (in pixels)	Error (%)
Phantom Unrotated	**9198**		
LA taken at the center		8564	6.9
Phantom at an angle	**10848**		
LA1(1) ONLY		8547	21.2
LA1(2) ONLY		8595	20.7
LA1(1) fused with LA1(2) (uncorrected)		10307	4.9
LA1(1) fused with LA1(2) (corrected)		10150	6.4
Real Data Simulation	**46162**		
LA1-fused ONLY		41798	9.5
LA2-fused ONLY		38200	17.2
LA1-fused and LA2-fused		46557	0.8

which is the lowest in uncorrected LA combination, could be misleading. That is why we also look at the shape of the output for qualitative validation.

4.2.2 Qualitative: Error in the shape of the output

In Figure 4.2 and Figure 4.3, the shape of the reference and estimated volume is shown. Although the quantative results for uncorrected LA combination case in phantom at an angle shows that the error is minimum, we observe that the shape of the estimate volume object in Figure 4.2 does not approximate the shape of the LA from base to apex. This is why for validating purposes, we look at both the percentage error and the shape of the estimated volume.

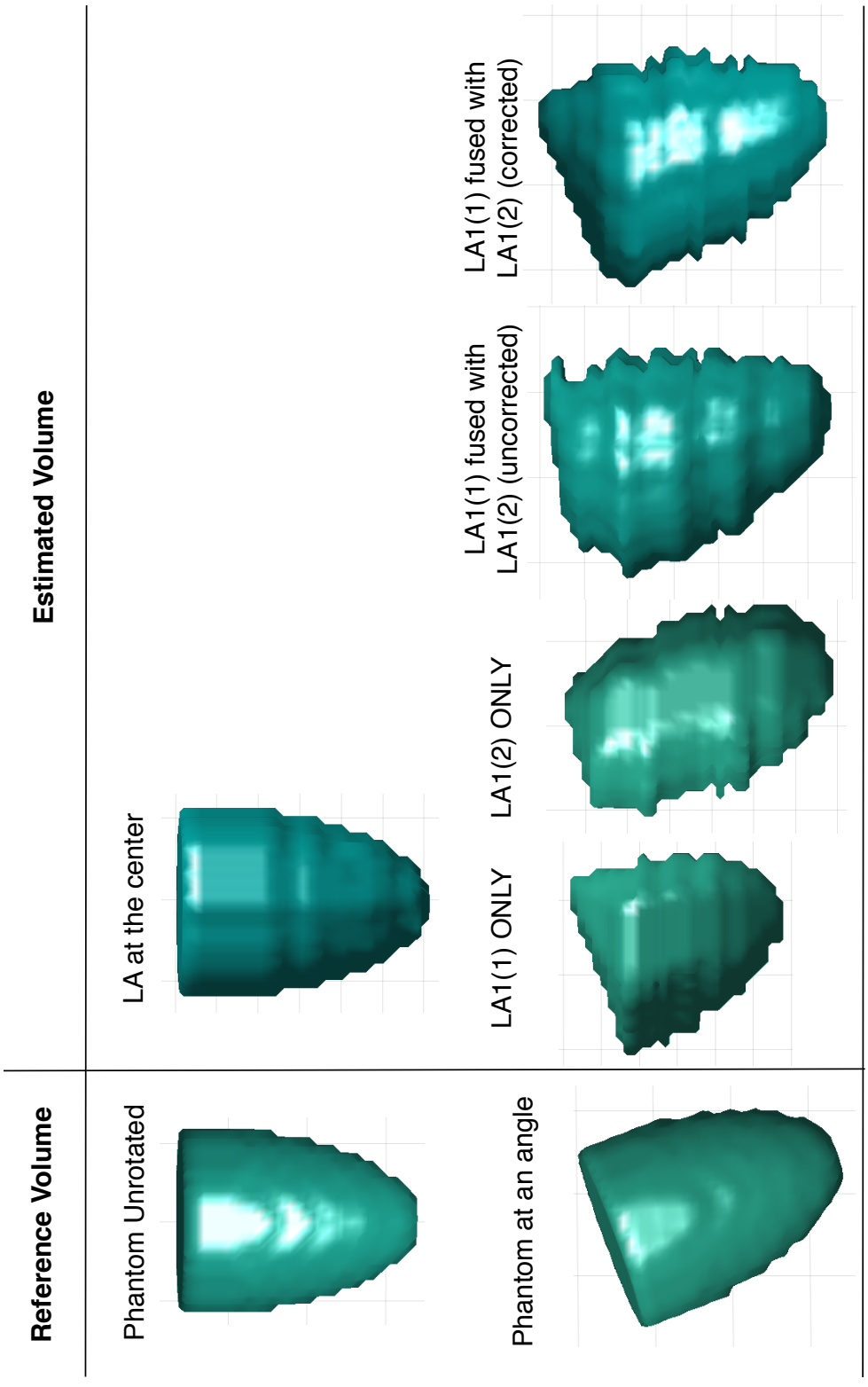

Figure 4.2: Shape of the volume estimated for phantom (unrotated) and phantom at an angle.

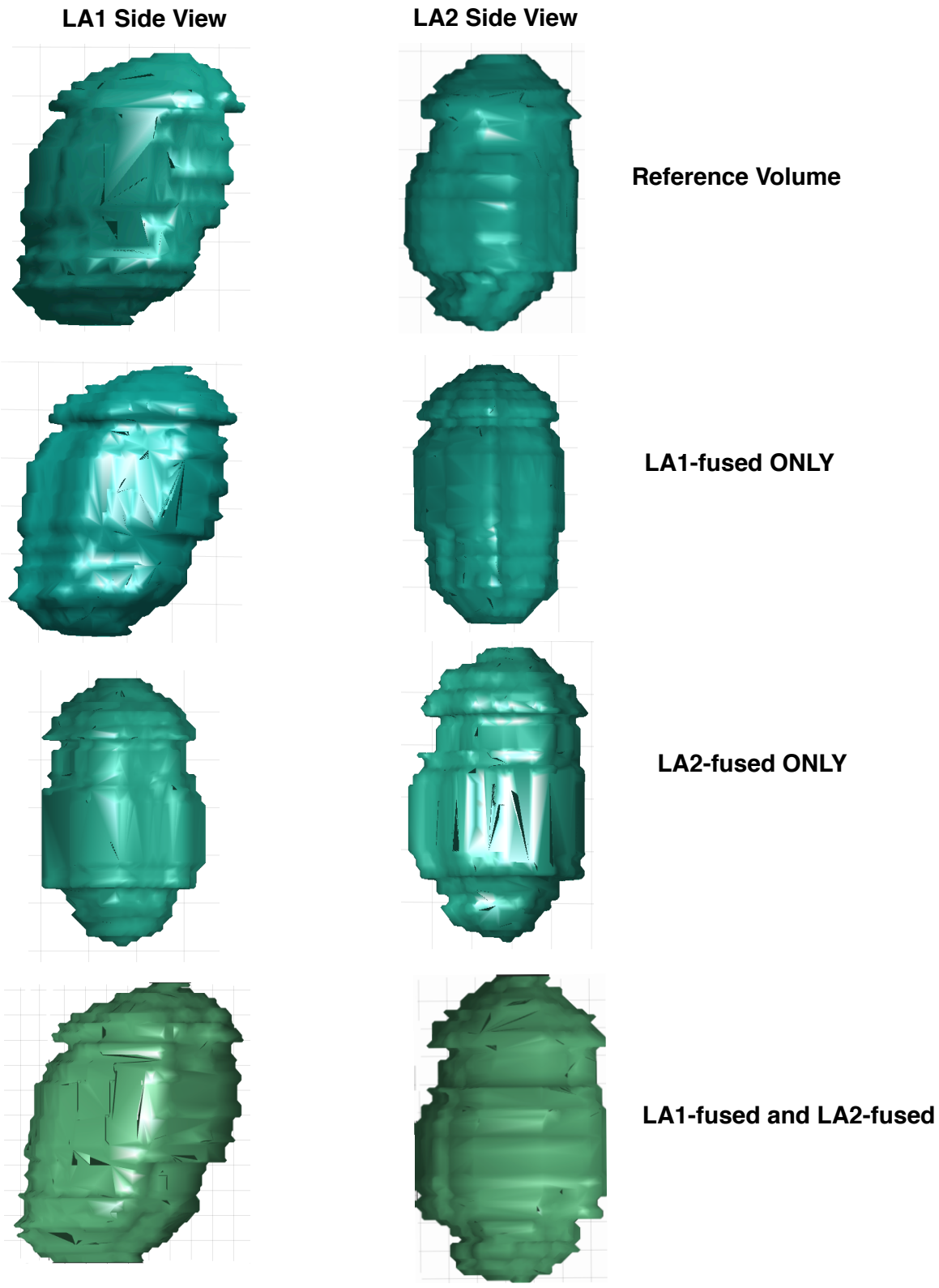

Figure 4.3: Shape of the volume estimated for non-uniform phantom object.

4.3 Given Data Volumetric

In this section, we will estimate volume for the given datasets using the slice-fitting method mentioned in the previous section. For the given data, we are given with the one LA slice and about 6-8 SA slices. We will however only utilize one SA slice and one LA slice (coronal) to estimate volume and compare that with the volume numbers given. As we have seen in the previous section for the Real Data Volumetric that if we use only one LA and one SA to compute volume, the error window lies between 10-20 percent. Knowing that error window size, we can expect this algorithm to fail if the given volume of two data being compared are with in 10-20 percent of each other, this algorithm might not be able to identify the difference.

The correlation between the given volume from slice-summation technique and the volume estimated using slice-fitting method was calculated using JMP software. In both cases, EDV and ESV as shown in Figure 4.4, the correlation was found to be greater than 0.5 and this is when we used only one LA and one SA slice to estimate volume. Using two LA slices and one SA slice, higher correlation is expected as the error goes down as per the results shown for a phantom volume computed in Table 4.1 using two LA slices and one SA slice.

Table 4.2: EDV data values (given vs estimated)

Serial#	File Name	Given Volume EDV(mL)	Given Volume (enlarged)	EDV Estimated (in pixels)
1	5691	0.037	37000	13062
2	5695	0.037	37000	29121
3	5696	0.031	31000	21761
4	5707	0.035	35000	19307
5	5710	0.035	35000	8478
6	5792	0.045	45000	23757
7	5797	0.057	57000	34579
8	5798	0.045	45000	24912
9	5799	0.044	44000	21957

Table 4.3: ESV data values (given vs estimated)

Serial#	File Name	Given Volume ESV(mL)	Given Volume (enlarged)	ESV Estimated (in pixels)
1	5691	0.01	10000	3400
2	5695	0.009	9000	5800
3	5696	0.011	11000	4773
4	5707	0.013	13000	4595
5	5710	0.011	11000	1798
6	5792	0.018	18000	7039
7	5797	0.023	23000	10122
8	5798	0.012	12000	4778
9	5799	0.014	14000	2959

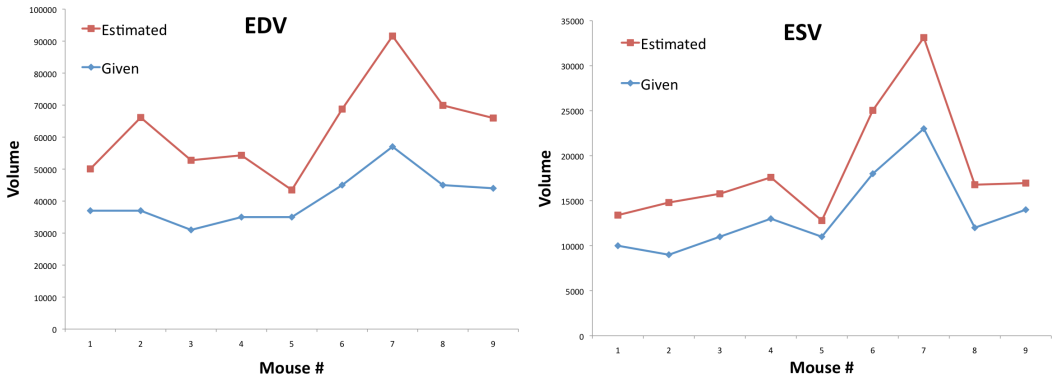

(a) EDV (b) ESV

Figure 4.4: Given volume (in blue from slice-summation) versus estimated (in red from slice-fitting) from 9 datasets showing how the volume results are correlated.

Chapter 5

Conclusion, Limitations and Future Work

5.1 Conclusion

From the outcomes of slice-fitting methodology discussed in Chapter 4, we can say that this method gives volume estimation of LV with in seven percent error difference if we use two orthogonal LA and one SA slice which significantly reduce (from 8 to 3) the number of slices required to compute volume. In this method, it does not matter whether the SA taken exactly parallel to MVP as long as it is orthogonal to the LA plane going from base to apex. We also demonstrated a technique of taking multiple LA slices and overlaying them in order to get a full profile of LA going from base to apex. This process eliminate the need for human intervention in determining the SA plane and make the imaging protocol independent of the experience level of data collector. In conclusion, the proposed slice-fitting method can succesfully replace the standard slice-summation technique.

5.2 Limitations

Although, the volume estimation seem to give good results, this method is based on the assumption that LV has ellipsoidal shape. This assumptions might not be true for ES phase where the apical region shown to have a greatest change in the shape. Moreover, the papillary muscles were included as a part of blood pool and not the myocardial muscle. Because otherwise, the endocardium boundary would not be able to work with the LV ellipsoidal shape assumption and may give us not only inaccurate but meaningless results.

5.3 Future Work

There are several other datasets that need to be tested using slice-fitting methodology. In future, the slice-fitting method can be applied to test how much variation in volumetric results we get if papillary muscle is included in blood pool or not. From the results of slice-fitting method and the techniques proposed to estimate LA from base to apex, imaging protocol can be changed in future mouse cardiac MRI studies to make use of slice-fitting methodology more efficient. To gain more confidence in the performance of this method, the results can be compared with some 3D MRI datasets that give more accurate results for volume than slice summation technique.

Bibliography

[1] Heart anatomy [online page]. retrieved on april 28th 2015 from http://www.texasheart.org/hic/anatomy/anatomy2.cfm.

[2] Robert S Balaban and Victoria A Hampshire. Challenges in small animal noninvasive imaging. *ILAR journal*, 42(3):248–262, 2001.

[3] D Saring, J Relan, M Groth, K Mullerleile, and H Handels. 3d segmentation of the left ventricle combining long-and short-axis mr images. *Methods of information in medicine*, 48(4):340, 2009.

[4] Si Yong Yeo, Liang Zhong, Yi Su, Ru San Tan, and Dhanjoo N Ghista. A curvature-based approach for left ventricular shape analysis from cardiac magnetic resonance imaging. *Medical & biological engineering & computing*, 47(3):313–322, 2009.

[5] James J Crowley, CL Huang, AR Gates, Anna Basu, Leonard M Shapiro, T Adrian Carpenter, and Laurance D Hall. A quantitative description of dynamic left ventricular geometry in anaesthetized rats using magnetic resonance imaging. *Experimental physiology*, 82(5):887–904, 1997.

[6] Cory M Swingen, Ravi Teja Seethamraju, and Michael Jerosch-Herold. Feedback-assisted three-dimensional reconstruction of the left ventricle with mri. *Journal of Magnetic Resonance Imaging*, 17(5):528–537, 2003.

[7] A Ardeshir Goshtasby and David A Turner. Fusion of short-axis and long-axis cardiac mr images. In *Mathematical Methods in Biomedical Image Analysis, 1996., Proceedings of the Workshop on*, pages 202–211. IEEE, 1996.

[8] Mostafa Ghelich Oghli, Alireza Fallahi, Vahab Dehlaghi, and Mohammad Pooyan. Left ventricle volume measurement on short axis mri images using a combined region growing and superellipse fitting method. *International Journal on Signal & Image Processing*, 4(2), 2013.

[9] Ying-Li Lu, Kim A Connelly, Alexander J Dick, Graham A Wright, and Perry E Radau. Automatic functional analysis of left ventricle in cardiac cine mri. *Quantitative imaging in medicine and surgery*, 3(4):200, 2013.

[10] Marwa MA Hadhoud, Mohamed I Eladawy, Ahmed Farag, Franco M Montevecchi, and Umberto Morbiducci. Left ventricle segmentation in cardiac mri images. *American Journal of Biomedical Engineering*, 2(3):131–135, 2012.

[11] C Constantinides, Y Chenoune, N Kachenoura, E Roullot, E Mousseaux, A Herment, and F Frouin. Semi-automated cardiac segmentation on cine magnetic resonance images using gvf-snake deformable models. *The MIDAS Journal-Cardiac MR Left Ventricle Segmentation Challenge*, 2009.

[12] Y Lu, P Radau, K Connelly, A Dick, and G Wright. Automatic image-driven segmentation of left ventricle in cardiac cine mri. *The MIDAS Journal*, 49:2, 2009.

[13] Michael R Kaus, Jens von Berg, Jürgen Weese, Wiro Niessen, and Vladimir Pekar. Automated segmentation of the left ventricle in cardiac mri. *Medical image analysis*, 8(3):245–254, 2004.

[14] Amol Pednekar, Uday Kurkure, Raja Muthupillai, Scott Flamm, and Ioannis A Kakadiaris. Automated left ventricular segmentation in cardiac mri. *Biomedical Engineering, IEEE Transactions on*, 53(7):1425–1428, 2006.

[15] GJ Heatlie and K Pointon. Cardiac magnetic resonance imaging. *Postgraduate medical journal*, 80(939):19–22, 2004.

[16] Nasser H Kashou. A practical guide to an fmri experiment. 2014.

[17] Marcello Ricardo Paulista Markus, Humberto Felício Gonçalves de Freitas, Paulo Roberto Chizzola, Gisela Tunes da Silva, Antonio Carlos Pedroso de Lima, and Alfredo José Mansur. Left ventricular mass in patients with heart failure. *Arquivos brasileiros de cardiologia*, 83(3):227–231, 2004.

[18] Carlos D Libhaber, Gavin R Norton, Muzi J Maseko, Olebogeng HI Majane, Aletta ME Millen, Fabian Maunganidze, Frederic S Michel, Richard Brooksbank, Elena Libhaber, Pinhas Sareli, et al. Relationship between inappropriate left ventricular hypertrophy and ejection fraction independent of absolute or indexed mass in a community sample of black african ancestry. *Journal of hypertension*, 31(1):169–176, 2013.

[19] Beverly H Lorell and Blase A Carabello. Left ventricular hypertrophy pathogenesis, detection, and prognosis. *Circulation*, 102(4):470–479, 2000.

Appendix A

Some real mice datasets SA slices boundaries are shown below that demostrate the trend from basal to mid to apical region as discussed earlier in section 3.1.

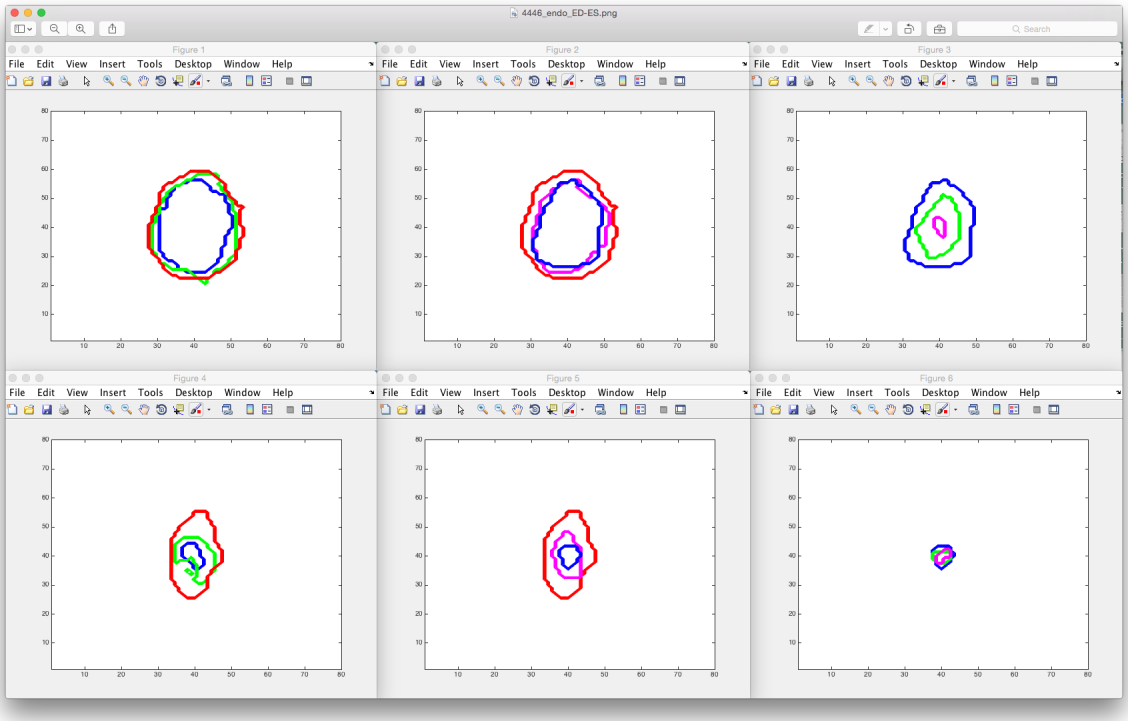

Figure A.1: Endocardial boundaries in mouse 4446 going from ED (top) to ES (bottom).

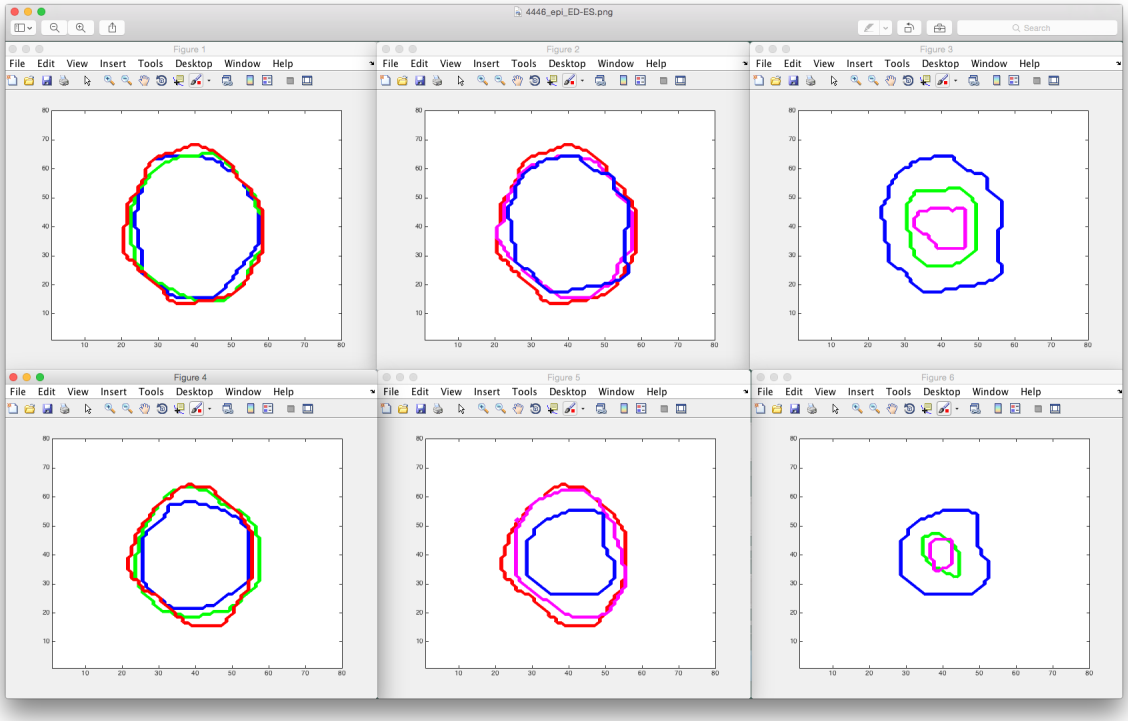

Figure A.2: Epicardial boundaries in mouse 4446 going from ED (top) to ES (bottom).

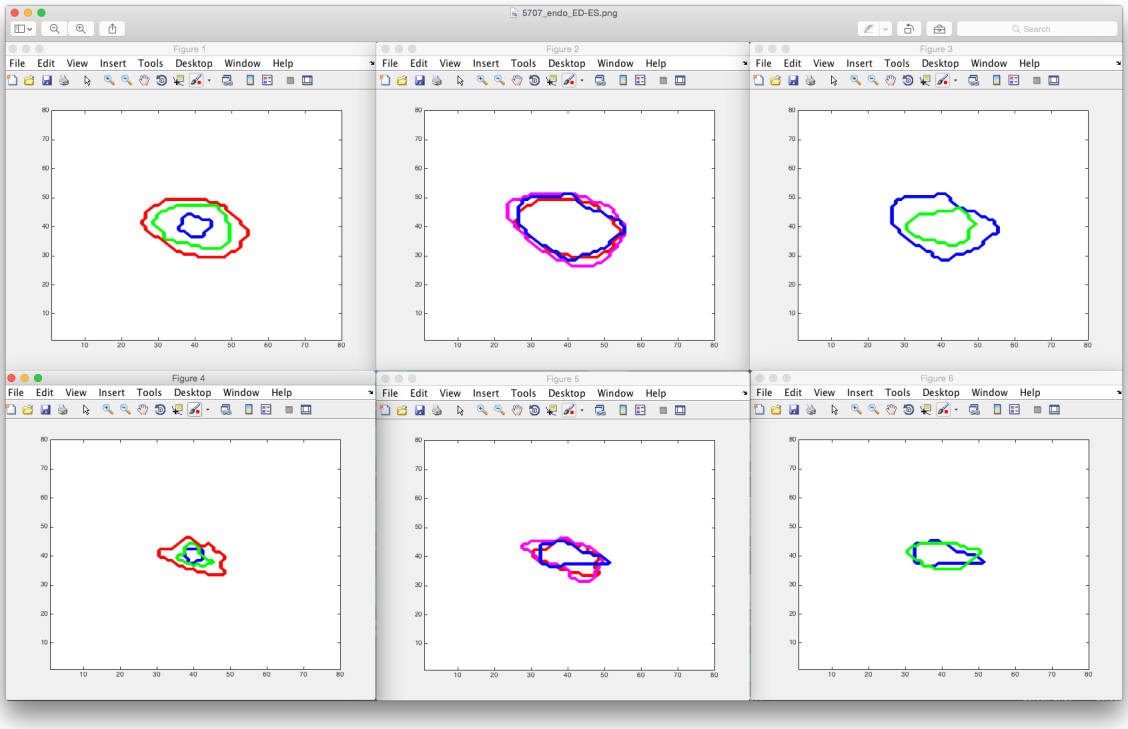

Figure A.3: Endocardial boundaries in mouse 5707 going from ED (top) to ES (bottom).

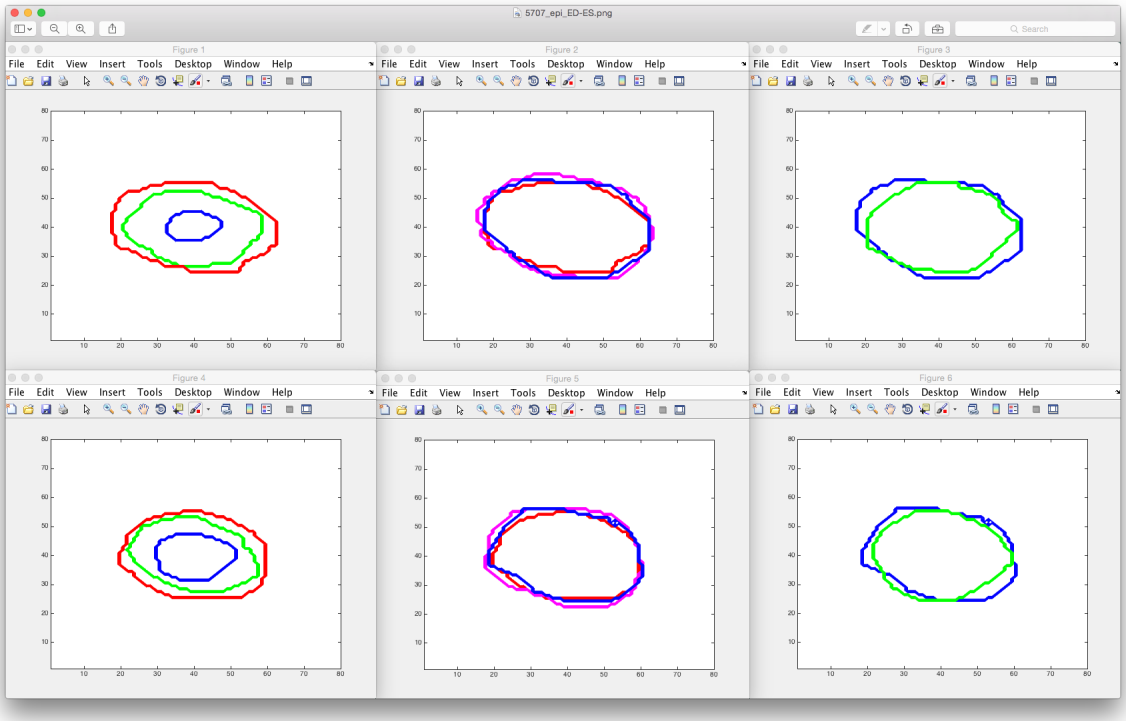

Figure A.4: Epicardial boundaries in mouse 5707going from ED (top) to ES (bottom).

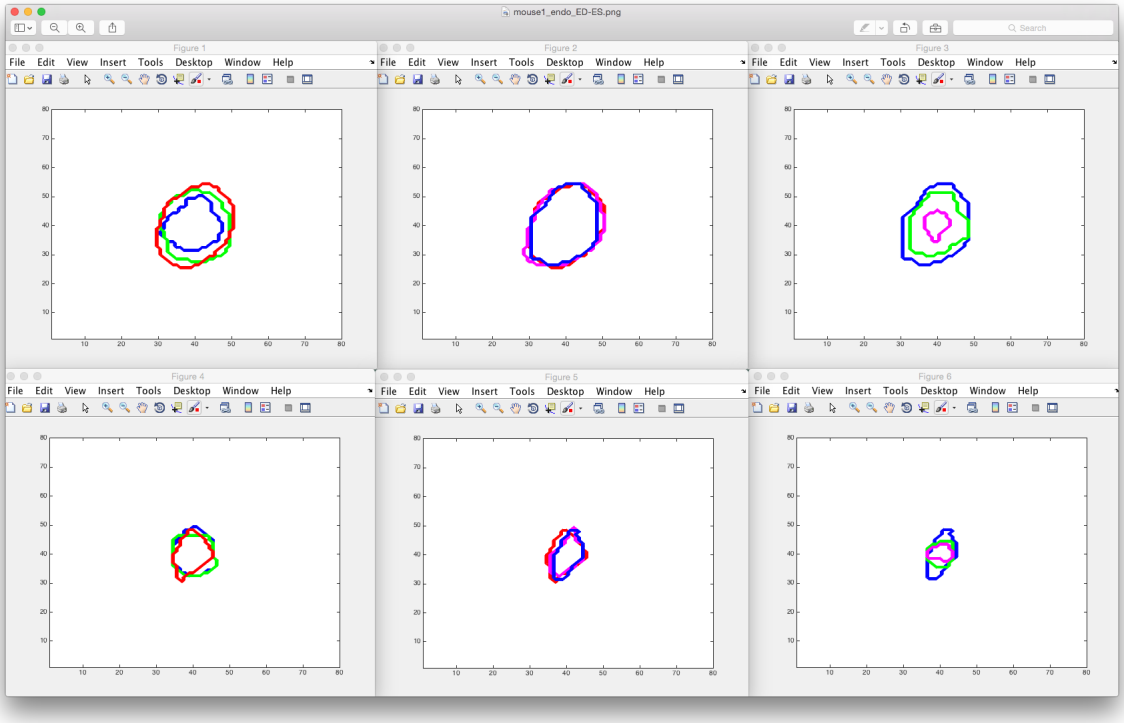

Figure A.5: Endocardial boundaries in mouse 1 going from ED (top) to ES (bottom).

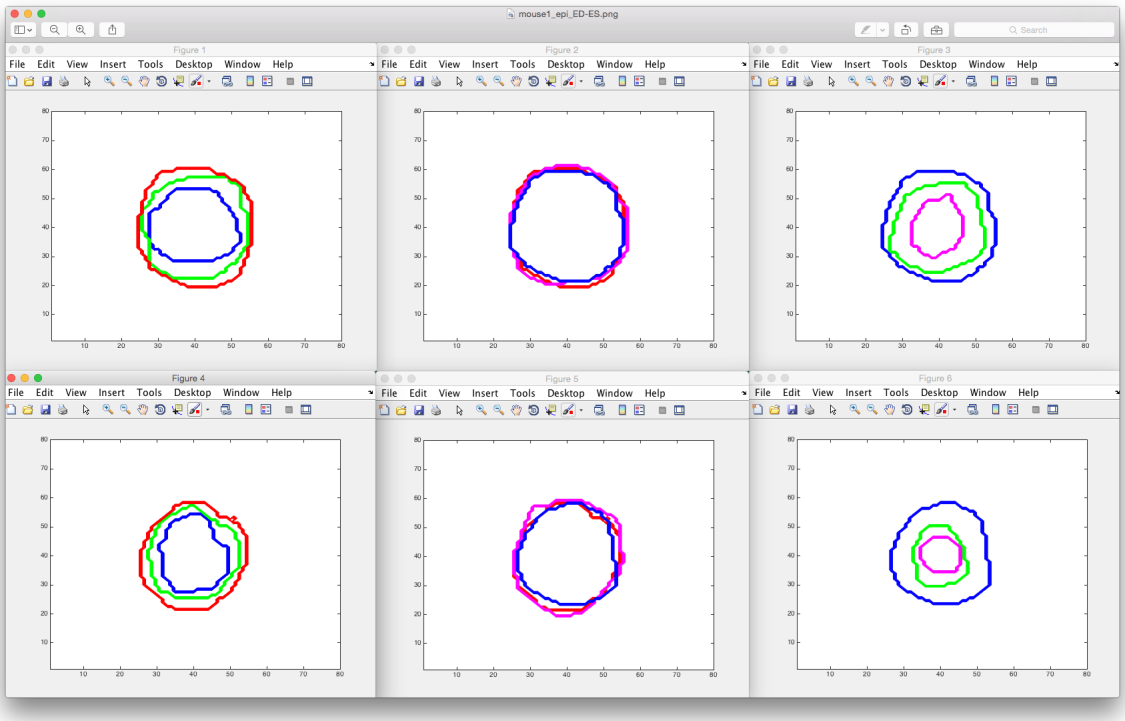

Figure A.6: Epicardial boundaries in mouse 1 going from ED (top) to ES (bottom).